

19.8 A 1.25mW 75dB-SFDR CT Filter with In-Band Noise Reduction

Antonio Liscidini, Alberto Pirola, Rinaldo Castello

University of Pavia, Pavia, Italy

In a direct-conversion wireless receiver the baseband filter should be able to handle large blockers, resulting in a very challenging spurious free dynamic range (SFDR) requirement. In particular, the noise added in-band trades off with the linearity required to handle close out-of-band interferers [1]. Since the integrated noise generally is proportional to kT/C , once the noise floor for the filter is set, the amount of capacitance is roughly defined as well as a lower bound for area and power consumption [2]. The solution presented in this paper aims to break this trade off by inserting an in-band zero in the output noise transfer function to improve the dynamic range.

The starting point of this work is the current-driven 1st-order LPF shown in Fig. 19.8.1. In this structure, the high impedance degeneration at low frequencies minimizes the noise injected by the cascode in the filter passband. As an analogy, the current signal flows as in a *pipe* where only losses or current injection can perturb the signal. Since in the passband, the filter behaves like a *lossless pipe*, no noise (or distortion) components can be added. In contrast, in the stopband the signal attenuation, provided by the capacitance, results in the corresponding increase of noise.

Furthermore, this filter also generates a small amount of distortion over the entire spectrum with the only exception of the transition region around the cutoff frequency. In fact, over the passband the circuit behaves like a *lossless pipe*, while out of band the signal is almost completely filtered out by the capacitance before entering in the nonlinear device. This combination of low in-band noise and high out-of-band linearity is very suitable for a wireless receiver baseband filter, because it maximizes the dynamic range just where the specifications are more constraining. However, for all of the above to be true, the output impedance for the signal source needs to be much higher than the $1/g_m$, i.e., the input impedance of the stage. Given the typical values of transistor transconductances, a large capacitance should be used to achieve the desired bandwidth. Moreover, channel selection needs filters with a sharp attenuation profile, mandating the use of complex-conjugate poles.

Low input impedance and complex-conjugate poles can be implemented using the schematic shown in Fig. 19.8.2. Setting the same transconductances for the stacked transistors, the loop around M1 produces a virtual ground at the input of the cell. At the same time, the structure behaves like a gyrator for the capacitance C2 that is seen as an inductance at the source of M1. This effect combined with the capacitance C1 realizes a pair of complex-conjugate poles.

Since the filter operates similar to a *lossless pipe* in the passband, the noise behavior of the cell closely resembles that of the single pole structure of Fig. 19.8.1, displaying a zero in the transfer functions of the noise of M1 and M2 that depends on the output impedance of the signal source. Figure 19.8.3 shows the noise contributions of M1 and M2, which are consistent with what described before. The total output noise is also shown where the minimum in-band noise is dominated by the bias circuit noise contributions.

As in the previous case, the signal is mainly filtered at the input of the stage resulting in a good linearity away from the cutoff frequency. Notice that, in both filters shown in Figs. 19.8.1 and 19.8.2, the highpass behavior of the output noise gives a total integrated in-band noise that is below kT/C . This is obviously not a violation of a fundamental limit but comes from the fact that the majority of the noise energy has been pushed outside of the band of interest.

To validate the theory, a 4th-order Butterworth LPF is implemented as a cascade of two biquadratic cells (NMOS and PMOS) as shown in Fig. 19.8.4. Two resistors (R1), in series with the sources of input devices, realize a linear V-I conversion. Although this is not required for proper circuit operation, this solution avoids the use of a linear transconductor, which would consume extra power. At the output of the second stage a differential resistance R2 transforms the current signal into voltage.

Particular attention is given to the design of bias current generators at the bottom and at the top of the structure since they are the dominant contributors of the in-band noise. This mandates the use of large overdrive for the devices that implement the current generators, which also increase their output impedance. The final results is a direct trade-off between the total in-band noise and the lowest voltage supply.

The filter, fabricated in a 90nm CMOS process, occupies 0.5mm², dominated by the low density (1.5ff/μm²) metal-insulator-metal capacitors. The total current draw is 500μA from a 2.5V supply. Figure 19.8.5 shows the measured frequency response and the output noise of the fabricated 4th-order Butterworth LPF. With the filter cutoff frequency of 2.8MHz, the output noise exhibits a minimum around 300kHz and in its passband, and a peak at the corner frequency which are consistent with both theory and simulation. The input-referred noise integrated over the UMTS channel bandwidth (from 4kHz to 2MHz) is 32μV_{rms} that becomes 37μV_{rms} when integrated across the entire filter bandwidth. The out-of-band linearity test is done injecting two tones at 10 and 19.5MHz (according to the UMTS standard) and results in an IIP3 of +36dBm. The out-of-band SFDR (as defined in [3]) is thus 75dB with a total power consumption of 1.25mW. A summary of measurement results and the prototype micrograph are reported in Figs. 19.8.6 and 19.8.7, respectively.

Acknowledgments:

This research has been supported by the Italian National Program FIRB, contract n° RBAP06L4S5. The authors want to thank Marvell for technology access and Steve Shia (TSMC) for his support.

References:

- [1] A. Yoshizawa and Y.P. Tsvividis, "Anti-Blocker Design Techniques for MOSFET-C Filters for Direct Conversion Receivers," *IEEE J. Solid-State Circuits*, vol. 37, no. 3, pp. 357-364, Mar., 2002.
- [2] G. Groenewold, "A High-Dynamic-Range Integrated Continuous-Time Bandpass Filter," *IEEE J. Solid-State Circuits*, vol. 27, no. 11, pp. 1614-1622, Nov., 1992.
- B. Razavi, *RF Microelectronic Circuits*, Prentice Hall, 1997.

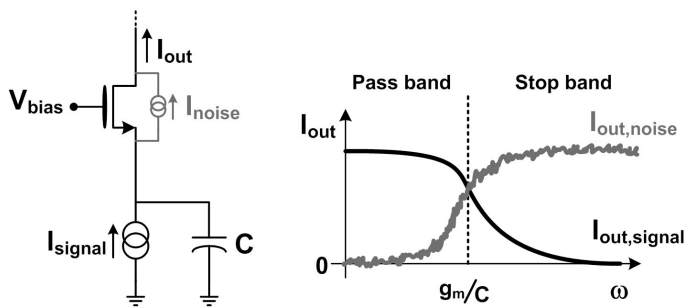
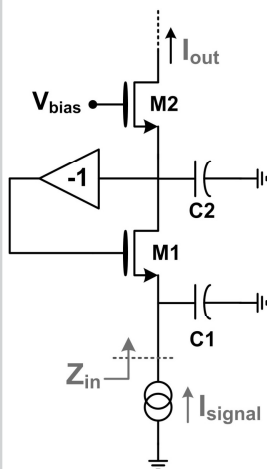


Figure 19.8.1: 1st-order LPF with in-band noise shaping.



$$\frac{i_{out}}{i_{in}} = \frac{g_m^2 / (C1 \cdot C2)}{s^2 + s(g_m / C1) + g_m^2 / (C1 \cdot C2)}$$

$$\omega_0 = \frac{g_m}{\sqrt{C1 \cdot C2}} \quad Q = \sqrt{\frac{C1}{C2}}$$

$$Z_{in} = \frac{s / C1}{s^2 + s(g_m / C1) + g_m^2 / (C1 \cdot C2)}$$

Figure 19.8.2: The presented biquadratic cell.

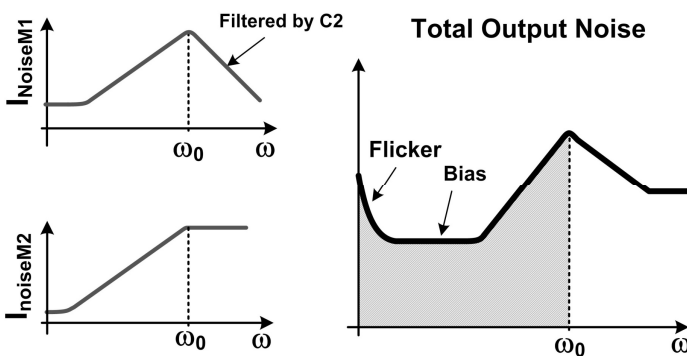


Figure 19.8.3: Biquadratic cell total output noise and M1 and M2 noise contributions.

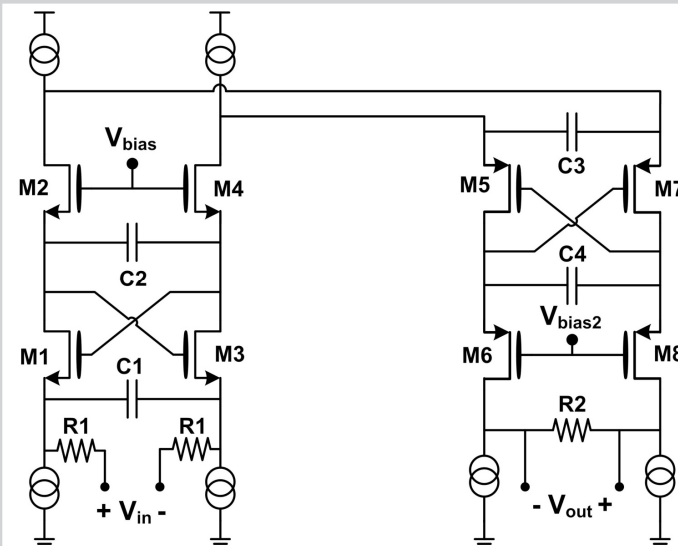


Figure 19.8.4: 4th-order Butterworth LPF.

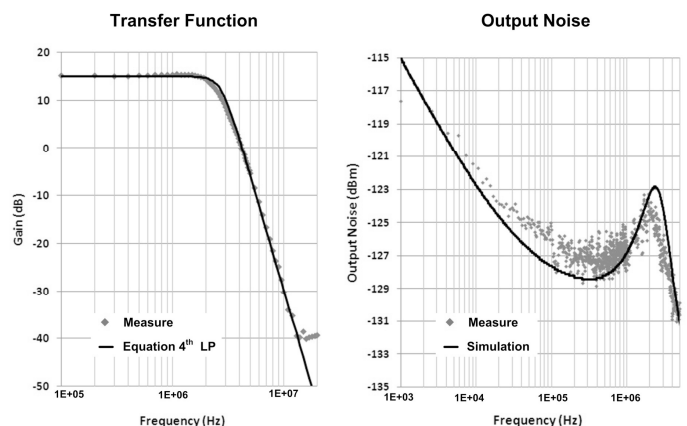


Figure 19.8.5: Measured filter transfer function and output noise spectral density.

Supply Voltage (V)	2.5
Power (mW)	1.25
Gain (dB)	15
Cutoff Frequency (MHz)	2.8
Order	4 th
Out-of-Band IIP3 (dBm)	36
Integrated Noise (μV_{rms})	32
Out-of-Band SFDR (dB)	75

Figure 19.8.6: Measured performance summary.

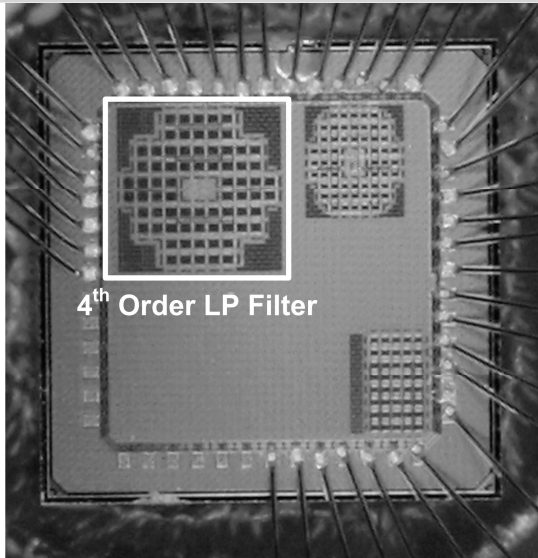


Figure 19.8.7: Chip micrograph.